OXFORD
SOT | Society of Toxicology
www.toxsci.oxfordjournals.org

TOXICOLOGICAL SCIENCES, 142(1), 2014, 6–20

doi: 10.1093/toxsci/kfu158
Advance Access Publication Date: August 4, 2014

AMP-Activated Protein Kinase Deficiency Rescues Paraquat-Induced Cardiac Contractile Dysfunction Through an Autophagy-Dependent Mechanism

Qiurong Wang*, Lifang Yang*,†, Yinan Hua*, Sreejayan Nair*, Xihui Xu*, and Jun Ren*,[1]

*Center for Cardiovascular Research and Alternative Medicine, University of Wyoming College of Health Sciences, Laramie, Wyoming 82071 and †Department of Anesthesiology, Xijing Hospital, Fourth Military Medical University, Xi'an 710032, China

[1]To whom correspondence should be addressed. Fax: (307) 766-2953. E-mail: jren@uwyo.edu.

ABSTRACT

Aim: Paraquat, a quaternary nitrogen herbicide, is a highly toxic prooxidant resulting in multi-organ failure including the heart although the underlying mechanism still remains elusive. This study was designed to examine the role of the cellular fuel sensor AMP-activated protein kinase (AMPK) in paraquat-induced cardiac contractile and mitochondrial injury. Results: Wild-type and transgenic mice with overexpression of a mutant AMPK α2 subunit (kinase dead, KD), with reduced activity in both α1 and α2 subunits, were administered with paraquat (45 mg/kg) for 48 h. Paraquat elicited cardiac mechanical anomalies including compromised echocardiographic parameters (elevated left ventricular end-systolic diameter and reduced factional shortening), suppressed cardiomyocyte contractile function, intracellular Ca^{2+} handling, reduced cell survival, and overt mitochondrial damage (loss in mitochondrial membrane potential). In addition, paraquat treatment promoted phosphorylation of AMPK and autophagy. Interestingly, deficiency in AMPK attenuated paraquat-induced cardiac contractile and intracellular Ca^{2+} derangement. The beneficial effect of AMPK inhibition was associated with inhibition of the AMPK-TSC-mTOR-ULK1 signaling cascade. *In vitro* study revealed that inhibitors for AMPK and autophagy attenuated paraquat-induced cardiomyocyte contractile dysfunction. Conclusion: Taken together, our findings revealed that AMPK may mediate paraquat-induced myocardial anomalies possibly by regulating the AMPK/mTOR-dependent autophagy.

Key words: paraquat; AMPK deficiency; autophagy; myocardium; contractile function

Autophagy is a highly coordinated intracellular lysosomal-mediated catabolic process that degrades damaged or dysfunctional proteins, cytoplasmic components, and intracellular organelles (Klionsky and Emr, 2000; Levine and Klionsky, 2004). It is essential to maintain cellular homeostasis in which removal of dysfunctional components and replacement with newly synthesized ones occurs dynamically. Autophagy can be turned on in response to starvation, protein aggregation, oxidative stress, and the damage that affects distinct cytoplasmic organelles (Levine and Klionsky, 2004; Niso-Santano *et al.*, 2011). It has been suggested that basal level of autophagy can be cardioprotective and play a pivotal role in the maintenance of cardiac geometry and function (Kuma *et al.*, 2004; Nakai *et al.*, 2007; Nemchenko *et al.*, 2011). Not surprisingly, autophagy can serve as a double-edged sword with both beneficial and detrimental effects in heart. Whereas certain studies have shown that autophagy may be protective in a number of heart diseases including ischemia-reperfusion injury and pressure overload-induced cardiac hypertrophy (Kassiotis *et al.*, 2009; Nakai *et al.*, 2007; Nemchenko *et al.*, 2011; Xu *et al.*, 2013a), others suggest that excessive or uncontrolled autophagy may lead to loss of functional protein, depletion of essential molecules, oxidative stress, collapse of cellular catabolic machinery, and ultimately autophagic cell death in the heart (Nemchenko *et al.*, 2011; Xie *et al.*, 2011).

Paraquat (1,1′-dimethyl-4,4′-bipyridinium dichloride), a widely used non-selective herbicide, is known to result in multiple organ damage and failure (Cristovao *et al*., 2009). Epidemiological studies have suggested that prolonged exposure of paraquat could increase the risk of developing Parkinson's disease in human subjects (Dagda *et al*., 2013; Liou *et al*., 1997). Paraquat, reminiscent of the dopaminergic neurotoxin MPP+, may deplete dopaminergic neurons in the midbrain, en route to apoptotic cell death (McCormack *et al*., 2002; Niso-Santano *et al*., 2006, 2011; Peng *et al*., 2004). A number of cellular mechanisms have been proposed for paraquat-induced cell injury including inhibition of mitochondrial oxidative phosphorylation and interruption of mitochondrial respiration chain, resulting in impaired energy metabolism, proteasomal dysfunction, and oxidative stress (Alexi *et al*., 2000; Gonzalez-Polo *et al*., 2004; McCormack *et al*., 2005; Niso-Santano *et al*., 2010; Tawara *et al*., 1996). Recent studies suggest that paraquat compromises myocardial survival and contractile function, en route to cardiopulmonary failure (Chan *et al*., 2007; Ge *et al*., 2010; Koo *et al*., 2002; Li *et al*., 2007). It has shown that paraquat could induce autophagy as evidenced by elevated autophagic markers such as Beclin-1, LC3 II, p62 degradation, and mammalian target of rapamycin (mTOR) dephosphorylation (Gonzalez-Polo *et al*., 2007; Niso-Santano *et al*., 2011). However, a number of neurological studies suggested that paraquat possibly promotes protein aggregation and blocks autophagy due to impaired basal autophagy (Garcia-Garcia *et al*., 2013; Manning-Bog *et al*., 2002, 2003). Nonetheless, whether and how autophagy is involved in paraquat-induced myocardial dysfunction still remains unclear.

The AMP-activated protein kinase (AMPK), a master regulator of several metabolic processes, acts as an autophagy inducer by directly phosphorylating TSC2 to activate the Rheb-GTPase, leading to suppressed mTOR complex 1 (mTORC1) and autophagy activation (Gottlieb, 2012; Inoki *et al*., 2003; Tripathi *et al*., 2013; Wullschleger *et al*., 2006). AMPK can also directly phosphorylate and activate unc-51-like kinase 1 (ULK1) to turn on autophagy independent of mTORC1 (Egan *et al*., 2011; Kim *et al*., 2011; Lee *et al*., 2010; Tripathi *et al*., 2013). However, activated ULK1 may participate in a negative feedback mechanism to suppress AMPK activity (Loffler *et al*., 2011). To this end, this study took advantage of a transgenic mouse model with overexpression of mutant AMPKα2 subunit to examine the impact of AMPK deficiency on paraquat-induced myocardial dysfunction and the underlying mechanisms with a special focus on autophagy.

MATERIALS AND METHODS

Experimental animals and paraquat treatment. All animal experimental procedures carried out here were approved by the Animal Use and Care Committees at the University of Wyoming (Laramie, WY). Adult muscle-specific AMPK kinase dead (KD) transgenic mice that express a KD rat α2 isoform (K45R mutation) and their wild-type (WT) littermates C57BL/6 were used as described (Mu *et al*., 2001; Russell *et al*., 2004). AMPK KD mice were genotyped using polymerase chain reaction (PCR) technique. The PCR primers used were: GGT CGA CGG TAT CGA TAA GCT TGA TAT C (forward) and GAA GGA ACC CGT TGG AGG ACT GGA GGC GAG G (reverse) (Mu *et al*., 2001; Turdi *et al*., 2011). All mice were housed in a temperature-controlled room (22.8 $\pm$ 2.0°C, 45–50% humidity) under a 12 h/12 h light/dark and allowed access to food and tap water *ad libitum*. For acute paraquat challenge, 4-month-old mice of both sex were delivered a single intraperitoneal injection of paraquat (45 mg/kg, ~100 μl, paraquat dichloride, Sigma-Aldrich, St. Louis, MO) or the vehicle saline, and were examined 48 h later (Day and Crapo, 1996). Body weight was recorded before and after treatment of paraquat or vehicle.

Echocardiographic assessment. Cardiac geometry and function were evaluated in anesthetized (ketamine 80 mg/kg and xylazine 12 mg/kg, i.p.) mice using the two-dimensional guided M-mode echocardiography (Philips SONOS 5500) equipped with a 15–6 MHz linear transducer. Left ventricular (LV) anterior and posterior wall dimensions during diastole and systole were recorded from three consecutive cycles in M mode using the method adopted by the American Society of Echocardiography. Fractional shortening was calculated from LV end-diastolic (LVEDD) and end-systolic (LVESD) diameters using the equation (LVEDD − LVESD)/LVEDD*100. Echocardiographic LV mass was estimated by $[(\text{LVEDD} + \text{septal wall thickness} + \text{posterior wall thickness})^3 - \text{LVEDD}^3] \times 1.055$, where 1.055 (mg/mm^3) is the density of myocardium. Heart rates were averaged over 10 consecutive cycles (Ren *et al*., 2008).

Cardiomyocyte isolation. After ketamine/xylazine sedation, hearts were rapidly removed from anesthetized 4-month-old adult mice of both sex and were mounted onto a temperature-controlled (37°C) Langendorff system. After perfusing with a modified Tyrode solution (Ca^{2+} free) for 2 min, the heart was digested for 16–20 min with a Ca^{2+}-free KHB buffer containing Liberase Blendzyme 4 (Hoffmann-La Roche Inc., Indianapolis, IN). The modified Tyrode solution (pH 7.4) contained the following (in mM): NaCl 135, KCl 4.0, $MgCl_2$ 1.0, HEPES 10, NaH_2PO_4 0.33, glucose 10, and butanedione monoxime 10, and the solution was gassed with 5% CO_2–95% O_2. The digested heart was then removed from the cannula and left ventricle was cut into small pieces in the modified Tyrode's solution. Tissue pieces were gently agitated and pellet of cells was resuspended. Extracellular Ca^{2+} was added incrementally back to 1.20 mM over a period of 30 min. A yield of at least 60–70% viable rod-shaped cardiomyocytes with clear sarcomere striations was achieved. Only rod-shaped cardiomyocytes with clear edges were selected for mechanical and intracellular Ca^{2+} studies (Li *et al*., 2007).

Cell shortening/relengthening. Mechanical properties of myocytes were assessed using a SoftEdge Myocam system (IonOptix Corporation, Milton, MA). IonOptix SoftEdge software was used to capture changes in cardiomyocyte length during shortening and relengthening. In brief, cardiomyocytes were placed in a Warner chamber mounted on the stage of an inverted microscope (Olympus IX-70) and superfused (~1 ml/min at 25°C) with a buffer containing (in mM) 131 NaCl, 4 KCl, 1 $CaCl_2$, 1 $MgCl_2$, 10 glucose, and 10 HEPES at pH 7.4. Myocytes were field stimulated with supra-threshold voltage at a frequency of 0.5 Hz (unless otherwise stated), 3 ms duration, using a pair of platinum wires placed on opposite sides of the chamber connected to a FHC stimulator (Brunswick, NE). The myocyte being studied was displayed on the computer monitor using an IonOptix MyoCam camera. IonOptix SoftEdge software was used to capture changes in cell length during shortening and relengthening. Cell shortening and relengthening were assessed using the following indices: peak shortening (PS)—the amplitude myocytes shortened on electrical stimulation, which is indicative of peak ventricular contractility; time-to-PS (TPS)—the duration of myocyte shortening, which is indicative of contraction duration; time-to-90% relengthening (TR_{90})—the duration to reach 90% relength-

ening, which represents cardiomyocyte relaxation duration (90% rather than 100% relengthening was used to avoid noisy signal at baseline concentration); and maximal velocities of shortening (+ dL/dt) and relengthening (− dL/dt)—maximal slope (derivative) of shortening and relengthening phases, which are indicatives of maximal velocities of ventricular pressure rise/fall (Ren *et al.*, 2008).

To assess the role of AMPK and autophagy in paraquat-induced cardiomyocyte contractile response, cardiomyocytes from adult WT mice were treated with paraquat (100 μM) at 37°C for 3 h (Ge *et al.*, 2010) in the presence or absence of the AMPK inhibitor compound C (5 μM) for 4 h (Guo and Ren, 2012), the mTOR inhibitor rapamycin (5 μM) for 4 h (Yuan *et al.*, 2009), the lysosomal inhibitor bafilomycin A1 (100 μM) for 2 h (Xu *et al.*, 2013b), or the autophagy inhibitor 3-methyladenine (3-MA, 10 mM) for 4 h (Guo and Ren, 2012).

Intracellular Ca^{2+} transients. A cohort of myocytes was loaded with fura-2/AM (0.5 μM) for 10 min and fluorescence intensity was recorded with a dual-excitation fluorescence photomultiplier system (Ionoptix). Myocytes were placed onto an Olympus IX-70 inverted microscope and imaged through a Fluor × 40 oil objective. Cells were exposed to light emitted by a 75W lamp and passed through either a 360 or a 380 nm filter, while being stimulated to contract at 0.5 Hz. Fluorescence emissions were detected between 480 and 520 nm and qualitative change in fura-2 fluorescence intensity (FFI) was inferred from FFI ratio at the two wavelengths (360/380). Fluorescence decay time (both single and bi-exponential decay rates) was measured as an indication of intracellular Ca^{2+} clearing rate.

Measurement of mitochondrial membrane potential ($\Delta\Psi m$). Mitochondrial membrane potential was measured using JC-1 (Invitrogen, T-3168) staining as described (Xu *et al.*, 2013a). Cardiomyocytes (~50 cells/mouse, 3 mice/group) that were isolated from WT and KD mice with or without paraquat treatment were seeded on gelatin-coated culture chamber slides and stained with JC-1 (5 μmol/l) at 37°C for 10 min. Cells then were washed with 1× PBS. Fluorescence of each sample was read at an excitation wavelength of 490 nm an emission wavelengths of 530 and 590 nm by a spectrofluorimeter (Spectra MaxGeminiXS, Spectra Max, Atlanta, GA). The aggregate form of JC-1 that yields high concentration of red fluorescence at ~590 nm indicates a healthy mitochondrial with normal membrane potential, whereas the monomer form of JC-1 which emitting low concentration of green fluorescence at ~530 nm. The fluorescence intensity results were evaluated by the ratio of 590-to-530-nm emission.

Western blot analysis. Heart tissues from study mice were homogenized and sonicated in a lysis buffer containing 20 mM Tris (pH 7.4), 150 mM NaCl, 1mM EDTA, 1 mM EGTA, 1% Triton, 0.1% sodium dodecyl sulfate, and a protease inhibitor cocktail. For *in vitro* study, isolated cardiomyocytes from WT mice treated with paraquat or rapamycin were sonicated in the lysis buffer as described above. Myocardial protein samples were incubated with anti-AMPK, anti-phosphorylated AMPK (pAMPK, Thr^{172}), anti-LC3B, anti-Beclin1, anti-TSC2, anti-phosphorylated TSC2 (pTSC2, Ser^{939}), anti-mTOR, anti-phosphorylated mTOR (pmTOR, Ser^{2448}), anti-S6K, anti-phosphorylated-S6K (pS6K, Ser^{792}), anti-ULK1, anti-phosphorylated ULK1 (pULK1, Ser^{777} and pULK1, Ser^{757}), anti-glyceraldehyde-3-phosphate dehydrogenase (GAPDH; loading control) (1:1000; Rabbit; Cell Signaling Technology, Danvers, MA), and anti-p62 (1:1000; Guinea Pig; Enzo Life Sciences, Plymouth Meeting, PA) antibodies. Protein samples from isolated cardiomyocytes were incubated with anti-Akt, anti-phosphorylated Akt (pAkt, Ser^{473}) and anti-glyceraldehyde-3-phosphate dehydrogenase (GAPDH; loading control) (1:1000; Rabbit; Cell Signaling Technology) antibodies. Horseradish peroxidase-coupled secondary antibodies were used for membrane incubation. After immunoblotting, the films were scanned and detected with a Bio-Rad calibrated densitometer and the intensity of immunoblot bands was normalized with corresponding band intensity of GAPDH (Ren *et al.*, 2009).

Data analysis. Data are mean ± SEM. Statistical significance ($p < 0.05$) for each variable was estimated by a one-way analysis of variance followed by Tukey's test for the post hoc analysis.

RESULTS

General Features and Echocardiographic Characteristics of WT and AMPK-KD Mice with or without Paraquat Treatment

Paraquat challenge overtly reduced body weight in WT mice compared with the vehicle injected counterparts. AMPK deficiency did not affect body weight. With the paraquat treatment, KD mice did not exhibit any significant decrease in body weight (Supplementary table 1S). Neither AMPK deficiency nor paraquat treatment overtly affected LV wall thickness and LVEDD. Paraquat treatment significantly reduced heart rate and fractional shortening whereas increased LVESD and LV mass/body weight ratio. Although AMPK deficiency did not exert any significant effect on these echocardiographic indices measured in the absence of paraquat treatment, it mitigated or significantly attenuated paraquat-induced change in these echocardiographic parameters (Fig. 1).

Effect of Paraquat Exposure and AMPK Deficiency on Cardiomyocyte Contractile Properties

Neither paraquat treatment nor AMPK deficiency affected cell length. However, cardiomyocytes from paraquat-treated WT mice displayed significantly reduced PS and ± dL/dt associated with unchanged TPS and TR_{90}. AMPK deficiency significantly abrogated paraquat-induced cardiomyocyte mechanical dysfunctions without eliciting any obvious effect by itself (Fig. 2).

Cardiomyocyte Intracellular Ca^{2+} Transient Properties

To explore the possible mechanism of action behind AMPK deficiency- and paraquat-induced cardiac responses, intracellular Ca^{2+} handling was evaluated using fura-2 fluorescence. Our data indicated that paraquat significantly suppressed the resting and peak intracellular Ca^{2+} levels (but not the rise in intracellular Ca^{2+}, Δ FFI), whereas it facilitated intracellular Ca^{2+} clearance. These changes of intracellular Ca^{2+} properties in response to paraquat were attenuated by AMPK deficiency. AMPK deficiency itself did not affect the electrically stimulated rise in intracellular Ca^{2+} (Δ FFI) (Fig. 3).

AMPK Deficiency Attenuates Paraquat-Induced Mitochondrial Dysfunction

As reported previously (Garcia-Garcia *et al.*, 2013; Gonzalez-Polo *et al.*, 2004, 2007; Niso-Santano *et al.*, 2011), paraquat challenge triggered mitochondrial injury. To evaluate the impact of AMPK deficiency on paraquat-induced mitochondrial injury, if any, mitochondrial function was assessed using JC-1 staining to monitor the mitochondrial membrane potential ($\Delta\Psi m$) in cardiomyocytes. Our results showed a significant reduction in the red, green fluorescence ratio in cardiomyocytes from paraquat-

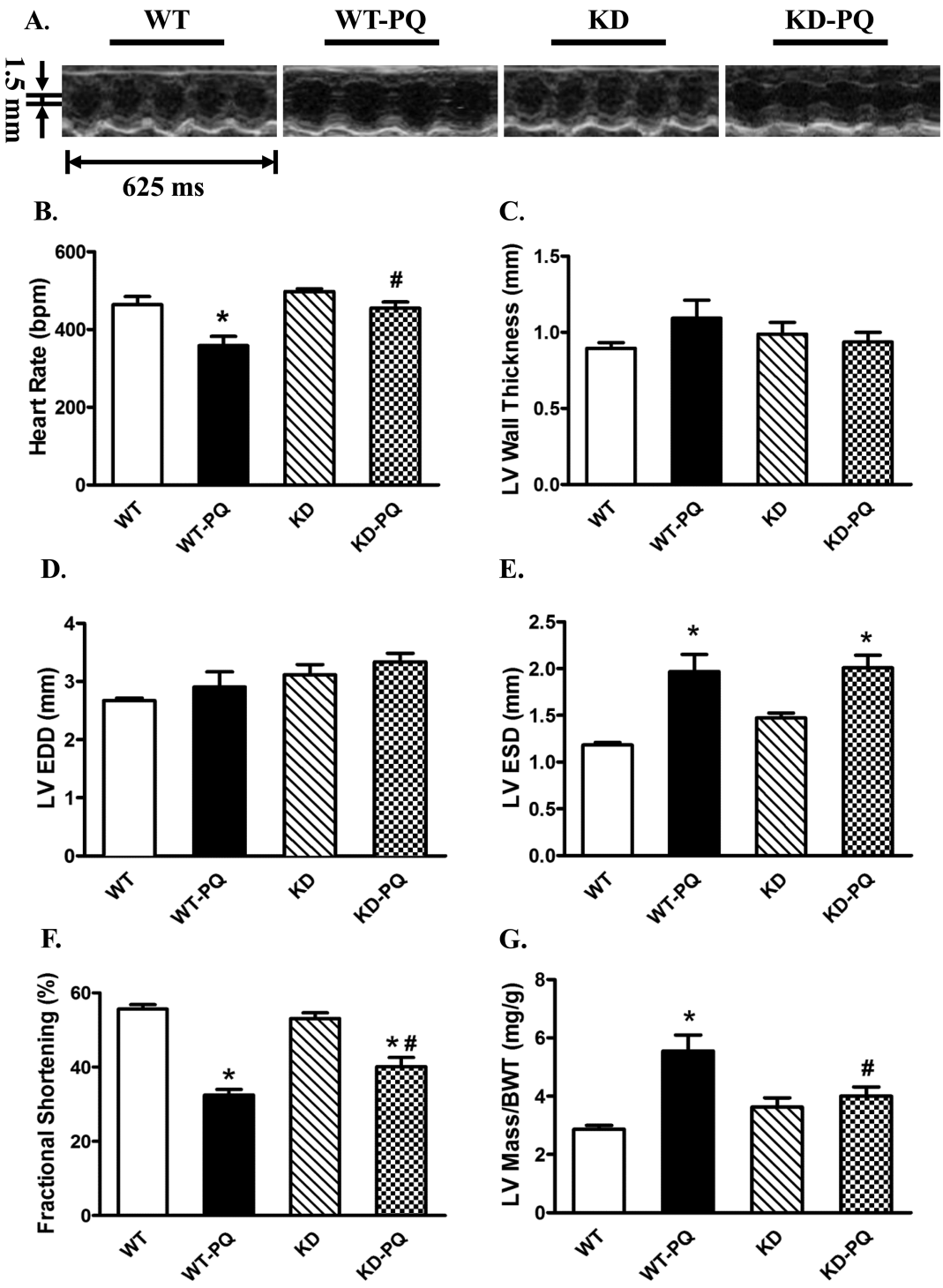

FIG. 1. Echocardiographic properties of WT and KD mice with or without treatment of paraquat (45 mg/kg, i.p.) or vehicle for 48 h. (A) Representative M-mode echocardiographic images from WT and KD mice treated with paraquat (45 mg/kg, i.p.) or vehicle for 48 h. (B) Heart rate (beat per minute); (C) LV wall thickness; (D) LV end diastolic diameter (EDD); (E) LV end systolic diameter (ESD); (F) fractional shortening (%); (G) calculated LV mass. Mean ± SEM, $n = 6$–8 mice per group; $^{*}p < 0.05$ versus WT group, $^{\#}p < 0.05$ versus WT-paraquat group.

treated WT mice, the effect of which was abrogated by AMPK deficiency. AMPK deficiency itself did not exert any significant effect on $\Delta\Psi m$ (Fig. 4).

Effect of Paraquat Exposure and AMPK Deficiency on Autophagy Markers

To explore the potential role of autophagy in paraquat-induced cardiac damage, levels of the autophagy markers Beclin-1, LC3I/II, and the cargo receptor p62 were evaluated by Western blot using myocardium from WT and KD mice following

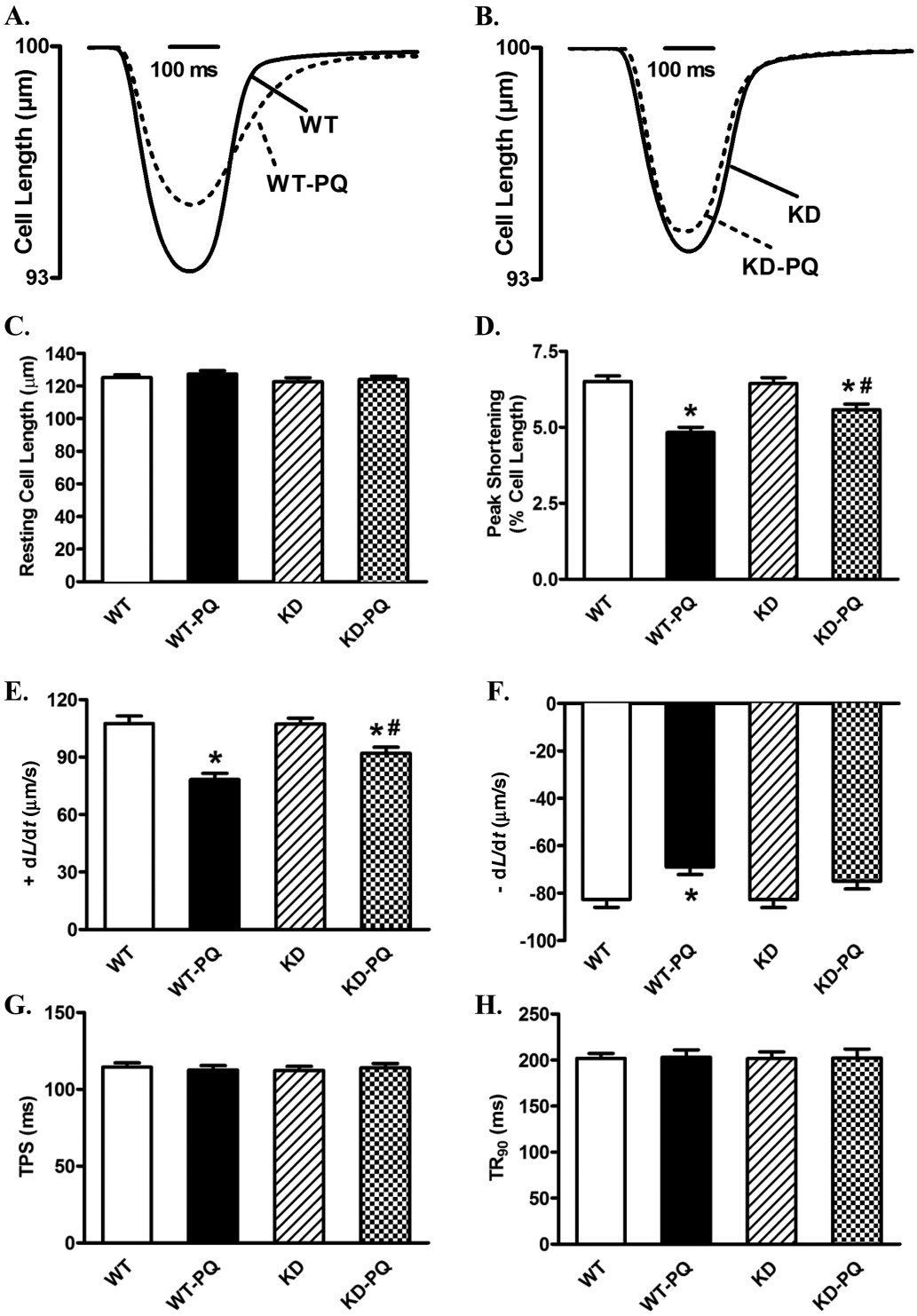

FIG. 2. Cardiomyocyte contractile properties in WT and KD transgenic mice treated with or without paraquat (45 mg/kg, i.p.) or vehicle for 48 h. (A) Representative traces from cardiomyocytes isolated from WT mice treated with paraquat (45 mg/kg, i.p.) or vehicle for 48 h. (B) Representative traces from cardiomyocytes isolated from KD mice treated with paraquat (45 mg/kg, i.p.) or vehicle for 48 h. (C) Resting cell length; (D) peak shortening (normalized to cell length); (E) maximal velocity of shortening (+ dL/dt); (F) maximal velocity of relengthening (− dL/dt); (G) time-to-peak shortening (TPS); (H) time-to-90% relengthening (TR_{90}). Mean ± SEM, $n = 114–141$ cells per group; $^{*}p < 0.05$ versus WT group, $^{\#}p < 0.05$ versus WT-paraquat group.

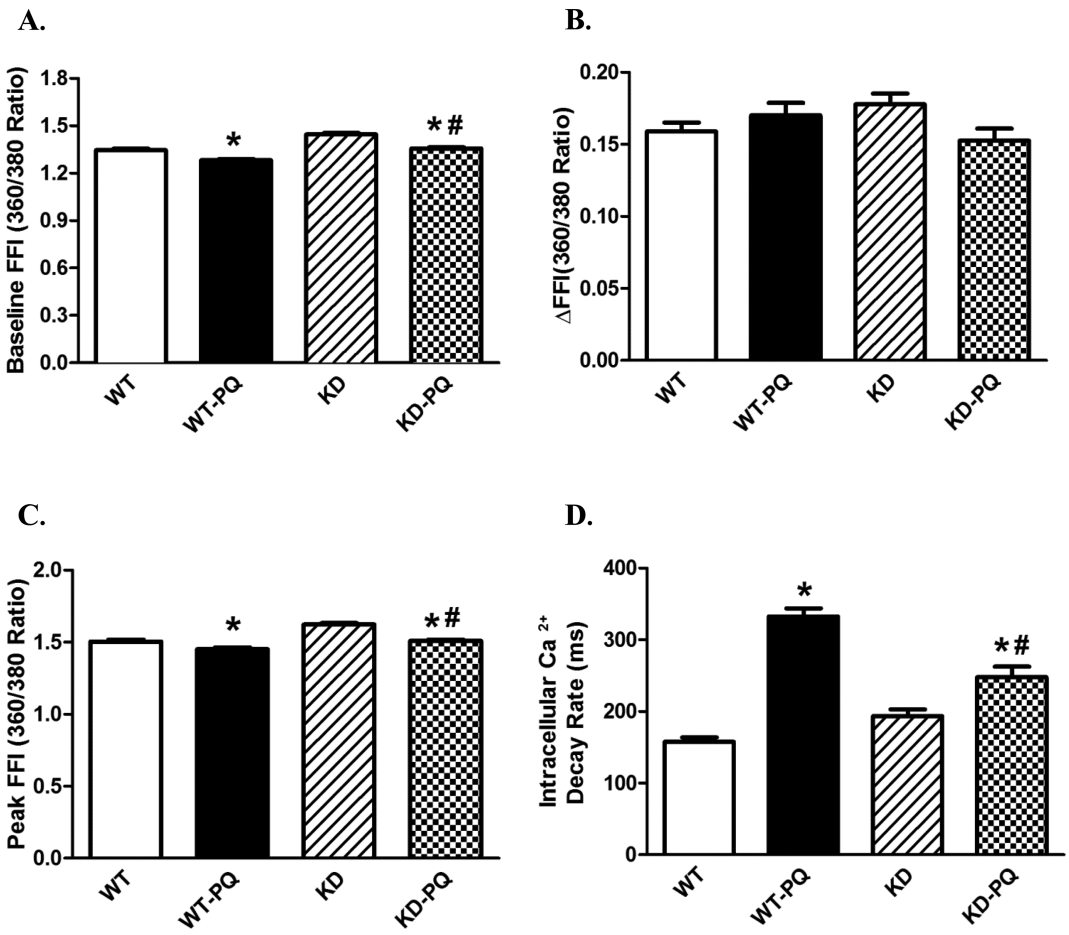

FIG. 3. Intracellular Ca^{2+} and frequency response in cardiomyocytes from WT and KD transgenic mice with or without paraquat (45 mg/kg, i.p.) or vehicle for 48 h. (A) Resting fura-2 fluorescence intensity (FFI). (B) Electrically stimulated rise in FFI (Δ FFI). (C) Peak fura-2 fluorescence intensity (peak FFI). (D) Single exponential intracellular Ca^{2+} decay. Mean ± SEM, $n = 79$–117 cells per group; $^{*}p < 0.05$ versus WT group, $^{\#}p < 0.05$ versus WT-paraquat group.

paraquat treatment. Our data suggested that paraquat treatment significantly elevated expression levels of Beclin1, LC3I, LC3II as well as the LC3II-to-LC3I ratio in WT mice. The expression level of p62 was significantly reduced in myocardium from paraquat-treated WT mice. Although AMPK deficiency itself did not affect the expression of these autophagy markers, it obliterated paraquat-induced changes in autophagy (Fig. 5).

Effect of Paraquat Exposure and AMPK Deficiency on AMPK-TSC-mTOR Signaling

To further consolidate the cell signaling mechanisms of AMPK deficiency in paraquat-induced autophagy, AMPK-related autophagic regulatory signaling molecules including TSC2, mTOR, S6K, and ULK1 were examined. Our data revealed reduced pan protein expression of AMPK in AMPK KD mice, validating the murine model (Figs. 6A and B). AMPK phosphorylation was significantly upregulated following paraquat treatment in WT mice, the effect of which was mitigated by AMPK deficiency. The AMPK downstream target, TSC2, was also examined. Our data revealed that paraquat dramatically increased myocardial TSC2 phosphorylation/activation (Figs. 6E–G). Meanwhile, phosphorylation of mTOR and S6K, as well as phosphorylation of ULK1 at Ser^{757}, was significantly dampened in the heart from paraquat-treated WT mice. However, phosphorylation of ULK1 at Ser^{777}, a downstream target regulated by AMPK, was elevated following paraquat treatment. Although AMPK deficiency itself failed to alter either pan or phosphorylated levels of these signaling molecules, it effectively attenuated paraquat-induced changes in these molecules (Fig. 7). Neither paraquat treatment nor AMPK deficiency showed any notable effect on pan expression of TSC2, mTOR, S6K, and ULK1 (Figs. 6 and 7).

Effect of AMPK Inhibitor Compound C, Rapamycin, Lysosomal Inhibitor Bafilomycin A1, and Autophagy Inhibitor 3-MA on Paraquat-Induced Cardiomyocyte Contractile Defects

To better elucidate a cause-effect relationship for AMPK and autophagy in paraquat-induced cardiac contractile response, freshly isolated cardiomyocytes from WT mice were exposed to paraquat in the presence or the absence of the AMPK inhibitor compound C, the mTOR inhibitor rapamycin, the lysosomal inhibitor bafilomycin, and the autophagy inhibitor 3-MA. Our data revealed that paraquat significantly depressed PS, maximal velocity of shortening/relengthening, and prolonged duration of relengthening without influencing resting cell length and duration of shortening. Although compound C and 3-MA themselves did not affect cardiomyocyte mechanical properties in the absence of paraquat exposure, they ablated or significantly attenuated paraquat-induced cardiomyocyte mechanical anomalies. However, the mTOR inhibitor rapamycin and lysosomal inhibitor bafilomycin exacerbated paraquat-induced cardiomyocyte contractile dysfunction. Combination of compound C with rapamycin further accentuated paraquat-induced con-

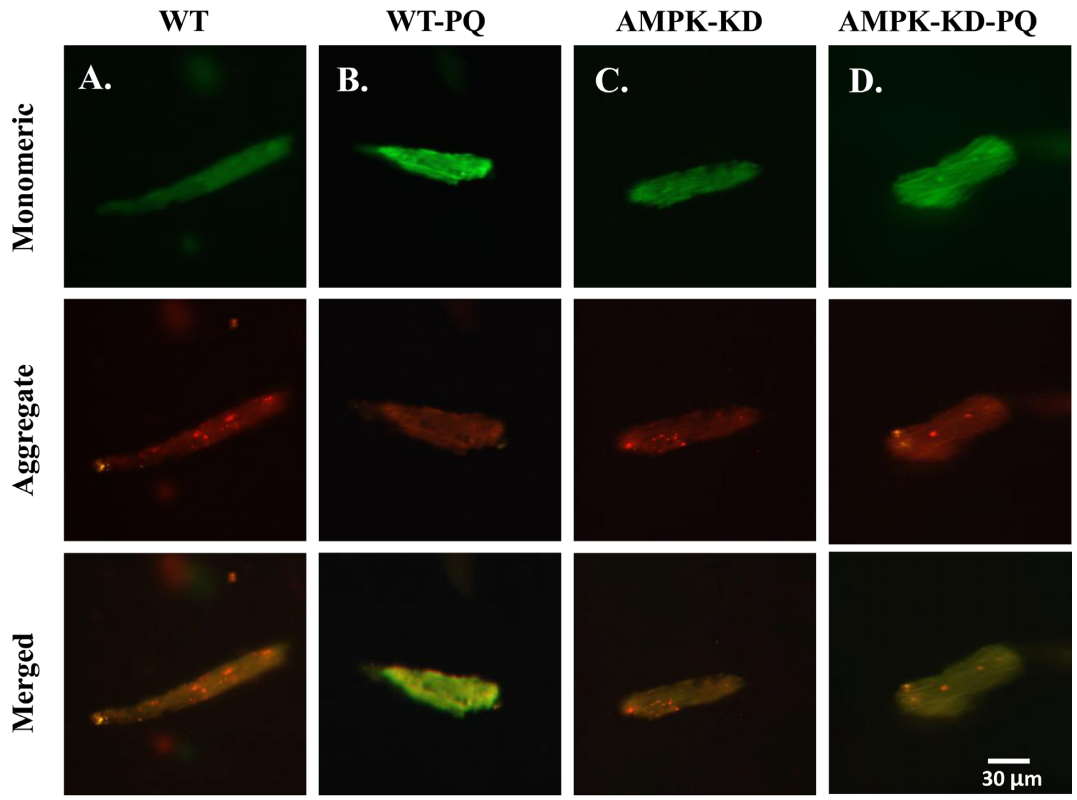

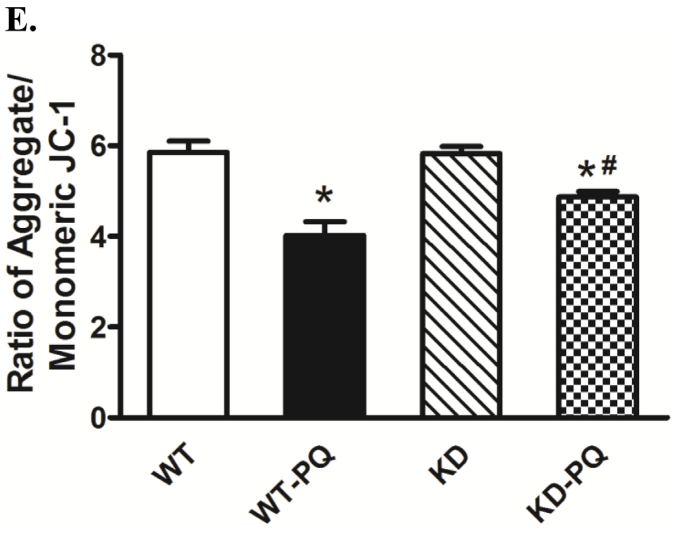

FIG. 4. JC-1 staining of cardiomyocytes (A through D, scale bar = 30 μM) from WT and KD mice treated with or without paraquat (45 mg/kg, i.p.) or vehicle for 48 h. (E) Quantitative analysis of the red/green fluorescence ratio (≈50 cardiomyocytes from three mice per group); $^{*}p < 0.05$ versus WT group, $^{\#}p < 0.05$ versus WT-paraquat group.

tractile dysfunction in cardiomyocytes. Nonetheless, combination of compound C and bafilomycin mitigated the paraquat-induced cardiomyocyte mechanical anomalies (Fig. 8). Furthermore, levels of pan and phosphorylated (Ser^{473}) Akt were measured in isolated cardiomyocytes treated with paraquat or rapamycin. Our results revealed that treatment of either paraquat or rapamycin did not affect pan or phosphorylated level of Akt (Supplementary fig. 1S).

DISCUSSION

The salient findings from our study suggested that AMPK deficiency significantly attenuated paraquat-induced damages in myocardial geometry and function, intracellular Ca^{2+} homeostasis, as well as mitochondrial injury (JC-1 fluorescence). Our data further revealed activation of autophagy in response to paraquat exposure, the effect of which was reversed by AMPK deficiency. More importantly, our findings provided compelling evidence for

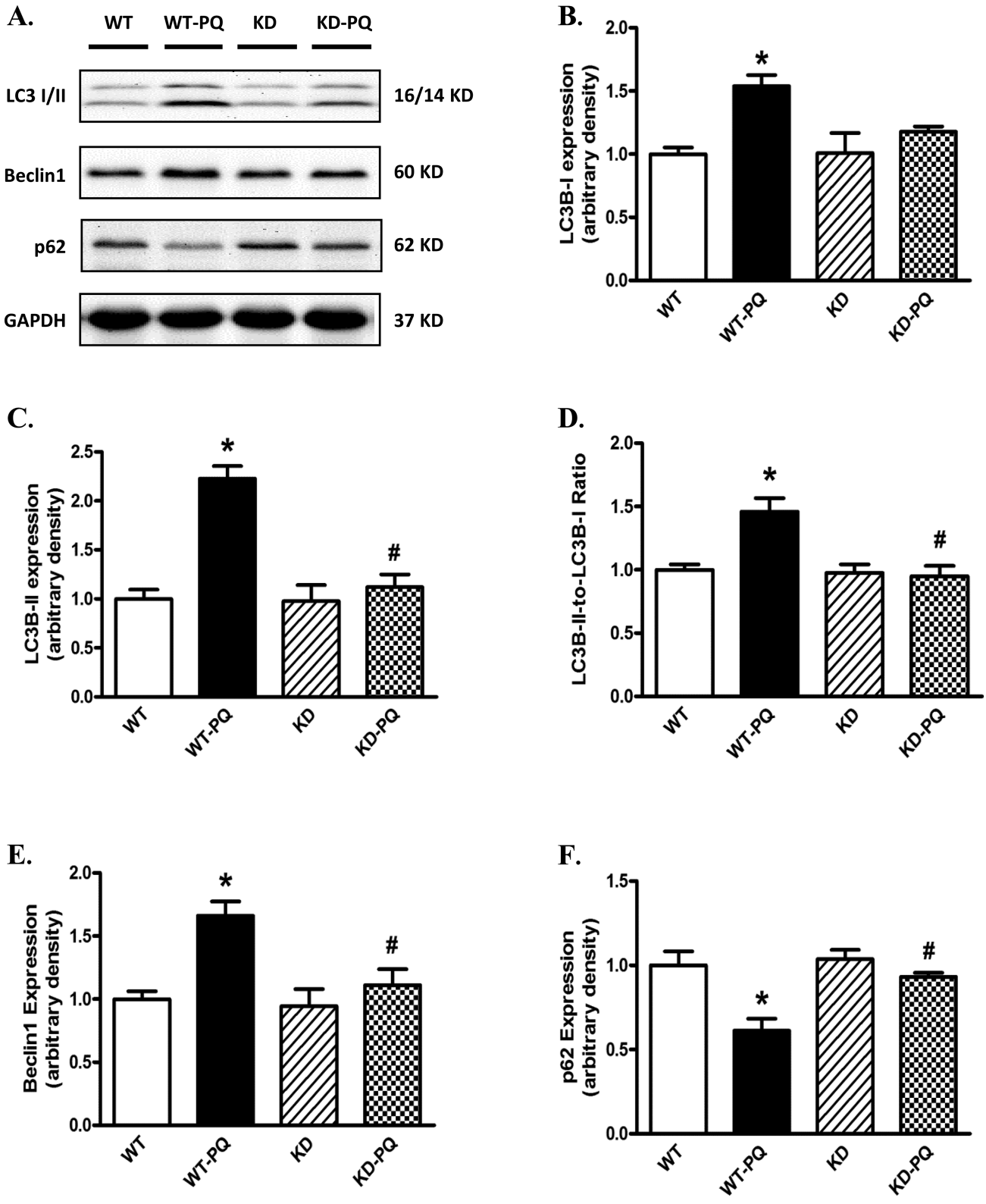

FIG. 5. Western blot analysis of autophagy markers in heart from WT and KD mice treated with or without paraquat (45 mg/kg, i.p.) or vehicle for 48 h. (A) Representative gel blots depicting LC3 I, LC3 II, p62, Beclin-2, and GAPDH (loading control) using specific antibodies. (B) LC3 I expression; (C) LC3 II expression; (D) LC3 II-to-LC3 I ratio; (E) Beclin-1 expression; and (F) p62 expression. Mean ± SEM, $n = 4–5$; $^{*}p < 0.05$ versus WT group, $^{\#}p < 0.05$ versus WT-paraquat group. Gel density of all groups was normalized with the respective gel density of WT group.

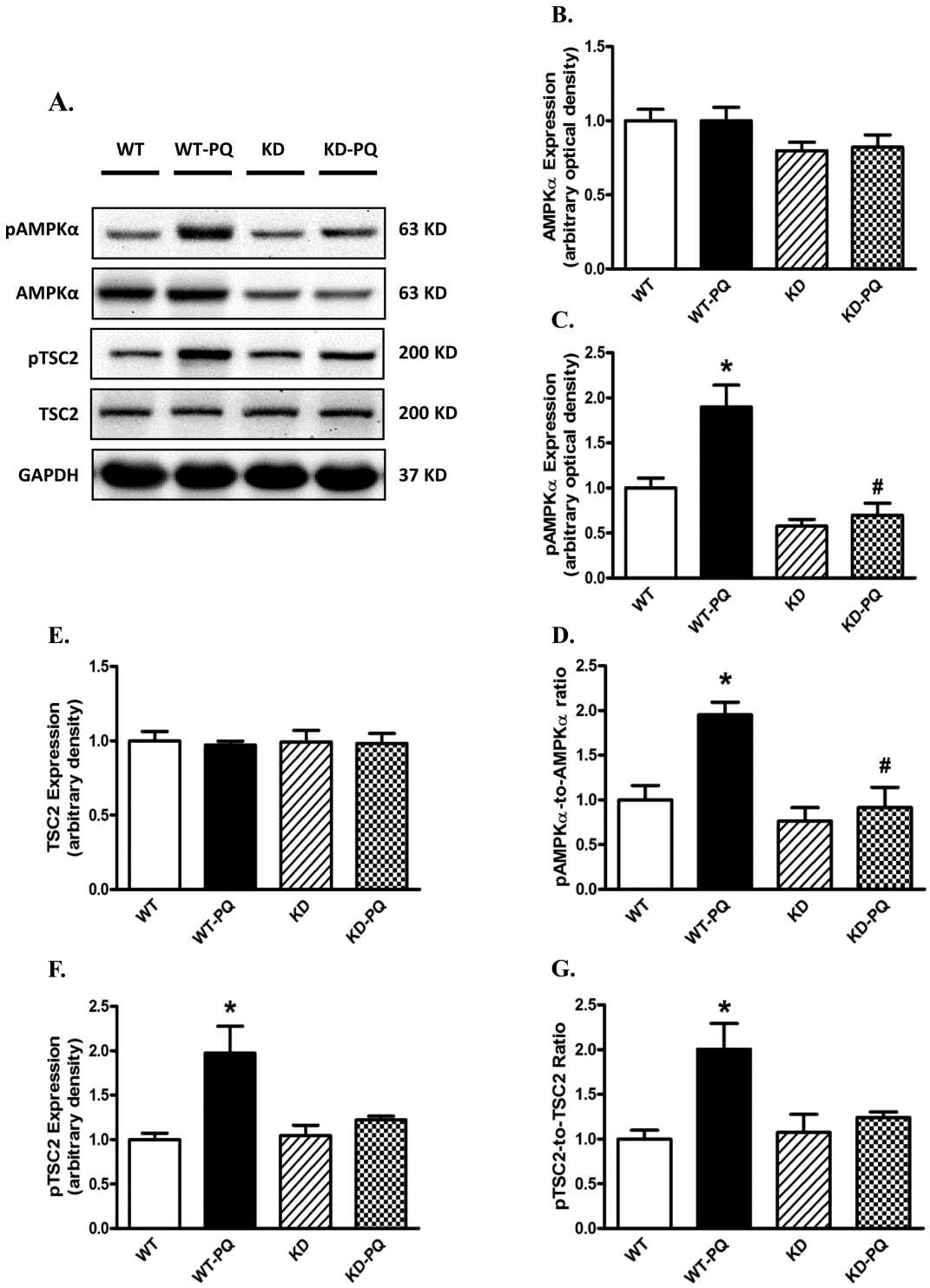

FIG. 6. Western blot analysis of AMPK-TSC signaling proteins from WT and KD mice treated with or without paraquat (45 mg/kg, i.p.) or vehicle for 48 h. (A) Representative gel blots depicting pan and phosphorylated AMPK, TSC2, and GAPDH (loading control) using specific antibodies; (B) AMPKα; (C) phospho-AMPKα (pAMPK, Thr^{172}); (D) pAMPKα-to-AMPKα ratio; (E) pan TSC2; (F) phospho-TSC2 (pTSC2, Ser^{939}); (G) pTSC2-to-TSC2 ratio. Mean ± SEM, $n = 4–5$; $^{*}p < 0.05$ versus WT group, $^{\#}p < 0.05$ versus WT-paraquat group. Gel density of all groups was normalized with the respective gel density of WT group.

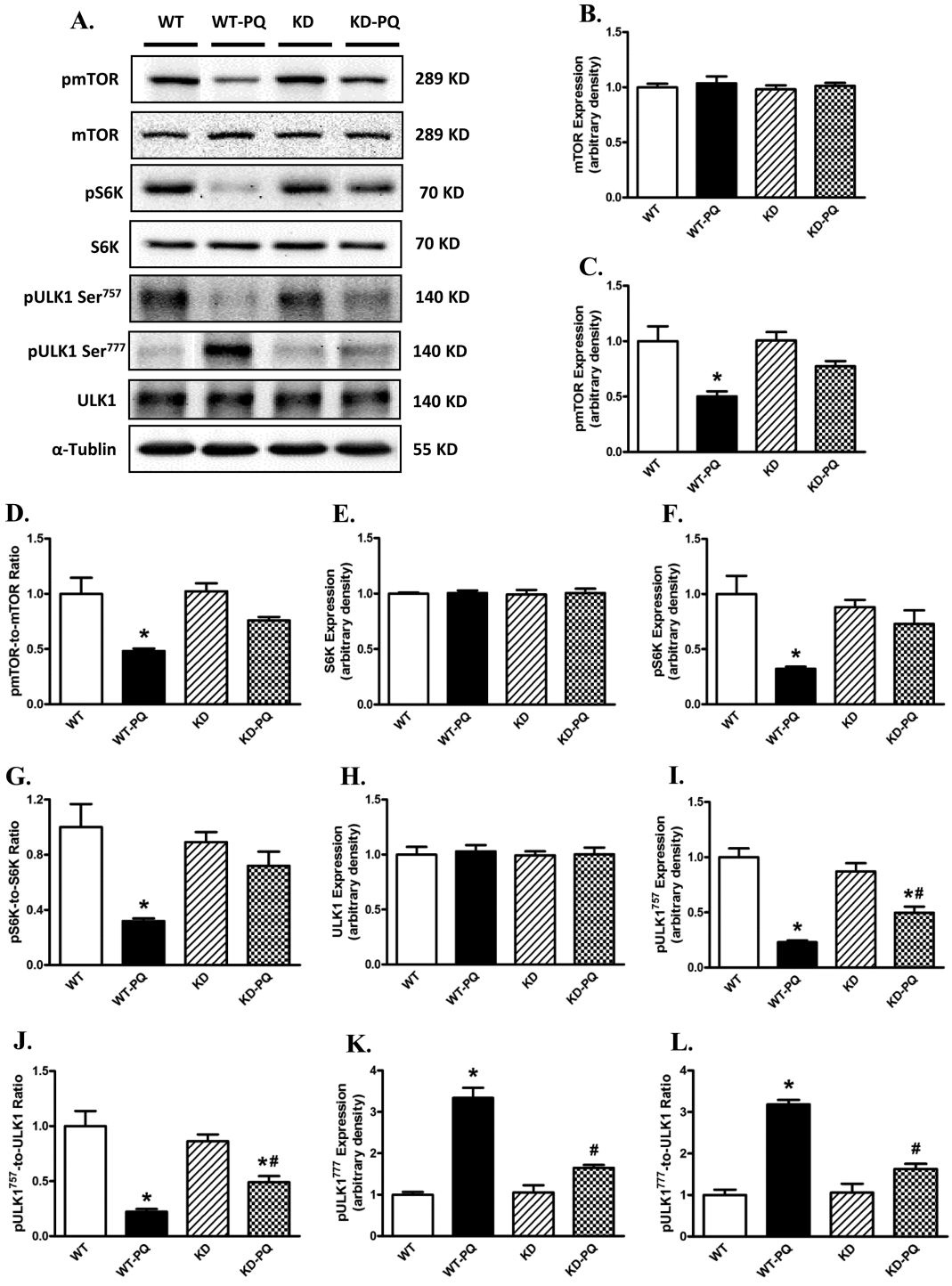

FIG. 7. Western blot analysis of mTORC1-related autophage signaling proteins from WT and KD mice treated with or without paraquat (45 mg/kg, i.p.) or vehicle for 48 h. (A) Representative gel blots depicting mTOR, phospho-mTOR (pmTOR, Ser^{2448}), S6K, phospho-S6K (pS6K, Ser^{792}), ULK1, phosphoULK1 (pULK1, Ser^{757} and pULK1, Ser^{777}), and α-tubulin (loading control) using specific antibodies; (B) pan mTOR; (C) pmTOR; (D) pmTOR-to-mTOR ratio; (E) pan S6K; (F) pS6K; (G) pS6K-to-S6K ratio; (H) pan ULK1; (I) pULK1 Ser^{757}; (J) $pULK1^{757}$-to-ULK1 ratio; (K) pULK1 Ser^{777}; (L) $pULK1^{777}$-to-ULK1 ratio. Mean ± SEM, $n = 4$–5, $^{*}p < 0.05$ versusWT group, $^{\#}p < 0.05$ versus WT-paraquat group. Gel density of all groups was normalized with the respective gel density of WT group.

a permissive role of the AMPK-TSC2-mTOR-ULK1 signaling in paraquat-elicited autophagy response, which may help to interpret paraquat-induced myocardial dysfunction. In addition, inhibition of AMPK and autophagy (compound C and 3-MA) protects against paraquat-induced cardiomyocyte contractile dysfunction. However, induction of autophagy by inhibiting mTOR (rapamycin) and impairment of autophagy flux by inhibiting lysosomal function (bafilomycin) exacerbated paraquat-induced cardiomyocyte contractile dysfunction. These observations are in favor of the notion that paraquat induces myocardial dysfunction through activation of autophagy via over-stimulation of AMPK and inhibition of mTOR.

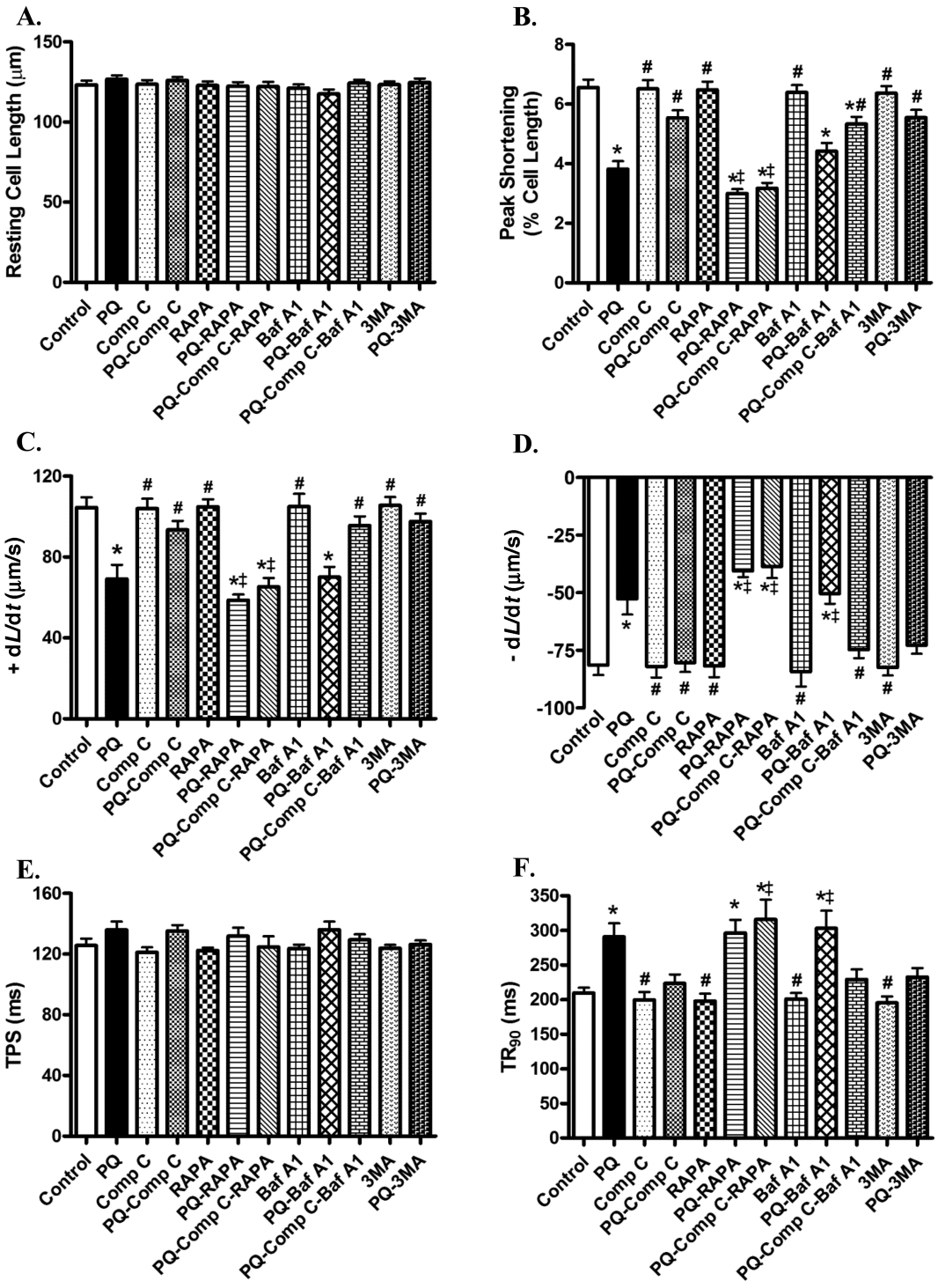

FIG. 8. Effect of compound C, rapamycin, bafilomycin A1, and 3-MA on paraquat-induced cardiomyocyte contractile defects. Freshly isolated cardiomyocytes from WT mice were incubated with paraquat (100 μM) in the presence or absence of the AMPK inhibitor compound C (5 μM), rapamycin (5 μM), lysosomal inhibitor bafilomycin A1 (100 nM), and 3-MA (10 mM) for 3 h. (A) Resting cell length; (B) peak shortening (normalized to resting cell length); (C) maximal velocity of shortening (+ dL/dt); (D) maximal velocity of relengthening (− dL/dt); (E) time-to-peak shortening (TPS); (F) time-to-90% relengthening (TR_{90}). Mean ± SEM, $n = 64$–157 cells from four mice per group; $^{*}p < 0.05$ versus control group, $^{\#}p < 0.05$ versus paraquat group, $^{\ddagger}p < 0.05$ versus paraquat compound C group.

The toxicity of paraquat has been intensively studied since 1960s (Bus *et al.*, 1976; Clark *et al.*, 1966). Mice have been used for a long time as a model to study the toxicity of paraquat (Day and Crapo, 1996; Day *et al.*, 1995; Giri *et al.*, 1981). Bus and colleagues reported a median lethal dose of paraquat for intraperitoneal injection at 30 mg/kg in mice (Bus *et al.*, 1976). Day and coworkers challenged mice with paraquat at 0, 35, 45, or 55 mg/kg for 48 h. In the 55 mg/kg treatment group, two out of five mice died prior to 48 h. All mice from other groups survived after 48 h of treatment (Day *et al.*, 1995). Moreover, Giri and colleagues found

significantly elevated pulmonary vascular permeability at 24 h and 48 h following paraquat treatment at 50 mg/kg (Giri *et al.*, 1981). Day and Crapo treated mice with 45 mg/kg paraquat intraperitoneal injection and studied the lung injury 48 h later (Day and Crapo, 1996). Based on these studies of paraquat in mice, we selected the dosage of 45 mg/kg i.p. for 48 h. Following the treatment, animal body weight was significantly decreased, whereas there was little significant change in body weight in KD mice. Our finding of weight loss is concordant with the previous report on paraquat toxicity in mice (Prasad *et al.*, 2009).

Our echocardiographic data showed that paraquat treatment significantly increased LVESD and LV mass-to-body weight ratio, as well as decreased fractional shortening. These findings are in line with the previous observations of myocardial dysfunction induced by acute paraquat treatment (Ge *et al.*, 2010; Li *et al.*, 2007). In addition, data from our study revealed that paraquat treatment triggered cardiomyocyte contractile dysfunction, as evidenced by reduced PS and maximal velocity of shortening/relengthening. Furthermore, intracellular Ca^{2+} homeostasis was disrupted in response to paraquat treatment, including depressed basal and peak intracellular Ca^{2+} levels and prolonged intracellular Ca^{2+} clearance. AMPK deficiency itself failed to elicit any notable change in cardiac geometry, cardiomyocyte contractile function, and intracellular Ca^{2+} handling properties, consistent with our previous reports (Guo and Ren, 2012; Turdi *et al.*, 2011). This finding suggests that AMPK deficiency may not be innately harmful to cardiac function (Guo and Ren, 2012; Musi *et al.*, 2005; Xing *et al.*, 2003). Nonetheless, overexpression of negative AMPKα2 subunit significantly ameliorated paraquat-induced cardiac remodeling, cardiomyocyte contractile dysfunction, and intracellular Ca^{2+} mishandling. These data indicate that AMPK may participate in the maintenance of intracellular Ca^{2+} homeostasis in cardiac pathological responses although the underlying mechanism remains unclear.

Our results further revealed that AMPK-TSC2-mTORC1-ULK1 signaling cascade played an essential role in paraquat-induced myocardial dysfunction. A robust increase in AMPKα phosphorylation was observed following paraquat treatment, which was reversed by AMPK deficiency. As the direct downstream target of AMPK and upstream regulator of mTORC1, TSC2 phosphorylation was also significantly elevated following paraquat exposure. It has been shown that mTORC1 is negatively regulated by TSC1/TSC2, whereas phosphorylation of TSC (aka, TSC1/TSC2 activation) inhibits mTORC1 en route to autophagy activation (Gottlieb, 2012; Xu *et al.*, 2014). In our hands, mTORC1 activity was significantly reduced in the paraquat-challenged mouse heart, a good indication for activated autophagy. AMPK deficiency was demonstrated to interrupt the inhibition of TSC2 on mTORC1 signaling, leading to phosphorylation of mTORC1 (Tripathi *et al.*, 2013). Accumulating studies have suggested that mTORC1 inhibition is an adaptive response during cardiac stress (Sciarretta *et al.*, 2014). It is consistent with our findings that *in vitro* treatment of rapamycin, a specific mTOR inhibitor, exacerbated paraquat-induced cardiomyocyte contractile dysfunction. Previous studies have shown that during acute treatment, rapamycin has a high specificity to inhibit mTORC1. However, chronic exposure of rapamycin may also inhibit mTORC2 (Lamming *et al.*, 2013). Moreover, mTORC2 is capable of further activating Akt through phosphorylation at Ser^{473} and therefore regulate Akt/mTORC1 signaling in a positive feedback loop (Efeyan and Sabatini, 2010; Fumarola *et al.*, 2014). For our short-term acute treatment of rapamycin in isolated cardiomyocytes, we did not observe any change in pan and phosphorylated (Ser^{473}) Akt in paraquat and rapamycin-treated

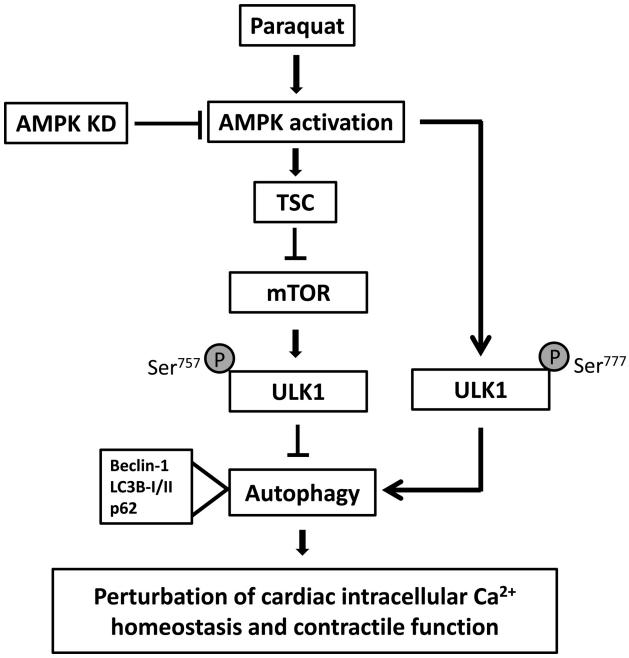

FIG. 9. Schematic diagram depicting possible mechanism(s) involved in paraquat- and AMPK deficiency (KD) induced changes in cardiac intracellular Ca^{2+} homeostasis and contractile function. Paraquat administration triggers activation of AMPK signaling. Activation of AMPK activates TSC complex (through phosphorylation) to enhance its inhibition on mTOR signaling and reduced phosphorylation of ULK1 at Ser^{757}, leading to excessive autophagy and autophagy flux, which leads to cardiac dysfunction. AMPK can alternatively activate ULK1 at Ser^{777} to upregulate autophagy. AMPK deficiency suppresses autophagy via inhibition of AMPK/TSC/mTOR/$ULK1^{757}$ and AMPK/$ULK1^{777}$ signaling cascade en route to cardioprotection. Arrows indicate activation whereas the lines with a "T" ending denote inhibition. TSC, tuber sclerosis complex.

groups. More importantly, autophagic protein ULK1/2, an essential regulator in the initiation process of autophagy, can be phosphorylated by either mTORC1 or AMPK (Ganley *et al.*, 2009; Sciarretta *et al.*, 2014). On one hand, our results revealed that ULK1 phosphorylation at Ser^{757} was significantly reduced following acute paraquat exposure, which is negatively regulated by AMPK (Bach *et al.*, 2011). On the other hand, we found that paraquat-induced distinct ULK1 phosphorylation at Ser^{777} was in concert with elevated AMPK phosphorylation, which was reversed by AMPK deficiency. It has been suggested that phosphorylation of ULK1 at Ser^{757} by active mTORC1 might prevent ULK1 from interacting with AMPK (Bach *et al.*, 2011). Dephosphorylation of ULK1 at Ser^{757} is thought to be enzymatically active and important for recruiting downstream autophagic proteins and subsequent autophagosome formation (Chan *et al.*, 2009; Guo and Ren, 2012). ULK1 can be regulated by multiple phosphorylation and dephosphorylation processes (Bach *et al.*, 2011). Studies have shown that AMPK can induce autophagy directly through phosphorylation of ULK1 at Ser^{317} and Ser^{777}, though other phosphorylation sites such as Ser^{555} and Ser^{467} may also participate in this process (Egan *et al.*, 2011; Kim *et al.*, 2011). A schematic diagram is provided to summarize the paraquat-induced autophagic and contractile responses through AMPK and TSC2, and subsequent inhibition of mTORC1 and phosphorylation of ULK1 (Fig. 9).

Our *in vivo* data revealed, for the first time, that AMPK deficiency or inhibition ameliorates paraquat-induced excessive autophagy in the heart manifested as increased expression level of both Beclin-1 and LC3 (LC3I and LC3II) and decreased autophago-

some cargo protein p62 along with contractile anomalies. These findings indicate that autophagy may play a causal role in paraquat-elicited cardiac damage possibly by over-activating autophagy, which was supported by *in vitro* findings that autophagy inhibition using 3-MA reversed mimicked paraquat-induced cardiomyocyte dysfunction. Moreover, *in vitro* treatment of rapamycin, which inhibits mTOR and activates autophagy, exacerbated cardiomyocyte dysfunction following the paraquat exposure, the effects of which were unaffected by AMPK inhibition. Similar effects were also observed in the cardiomyocyte contractile properties with the *in vitro* treatment of lysosomal inhibitor bafilomycin that blocks the autophagosome removal and resultant interruption of autophagic flux. However, AMPK inhibition effectively reversed these unfavorable effects. These findings suggest that autophagy activation is the key cause effect of paraquat-induced myocardial dysfunction; AMPK is a major regulator of paraquat-induced autophagy; impaired autophagic flux can also lead to cardiomyocyte contractile anomalies. It is possible that under AMPK deficiency or inhibition, autophagy is inactivated through either elevated mTORC1 activity (en route to elevated ULK1 Ser^{757} phosphorylation) or suppressed ULK1 Ser^{777} phosphorylation. These findings supported a crucial role of autophagy in paraquat-induced cardiac contractile dysfunction with over-activated AMPK, which suggests that autophagy induction may be detrimental in this process.

Perhaps, the most intriguing finding from our study is that autophagic flux plays an important role in cardiac response to pathological stress. Autophagic flux is the entire process of autophagy including the delivery of autophagosomal cargo to lysosome, degradation of autophagolysosome, as well as the release of the degradation product back into the cytosol. In responding to perturbations in the extracellular environment, cells have the ability to adjust autophagic flux to meet intracellular metabolic demands (Garcia-Garcia *et al*., 2013). A number of studies have shown that paraquat toxicity robustly increases the number of autophagic vacuoles or cause accumulation of autophagosomes (Garcia-Garcia *et al*., 2013; Gonzalez-Polo *et al*., 2007; Niso-Santano *et al*., 2010). Accumulation of autophagosomes can result from either increased autophagic flux or impaired autophagolysosome clearance (Garcia-Garcia *et al*., 2013). Paraquat has been reported to facilitate autophagy with improved autophagic flux (Gonzalez-Polo *et al*., 2007; Niso-Santano *et al*., 2010), whereas others show that paraquat impairs autophagic flux and the resulting protein accumulation (Garcia-Garcia *et al*., 2013; Wills *et al*., 2012). Here, we demonstrated that paraquat stimulates autophagic flux; meanwhile, our *in vitro* studies with treatment of bafilomycin, mimicking impaired autophagic flux, revealed that blocked autophagy can exacerbate the cardiomyocyte contractile dysfunction.

In conclusion, findings from our present study provided convincing evidence for the first time that AMPK deficiency helps to ameliorate paraquat-induced myocardial contractile dysfunction. Our data revealed a pivotal role of autophagy in cardiac stress response to environmental toxin paraquat, which may be possibly via AMPK-TSC2-mTORC1-ULK1-mediated regulation of autophagy. This is supported by the finding that inhibition of AMPK or autophagy protected against paraquat-induced cardiac anomalies. Although it is still premature to discern the precise mechanism underneath AMPK-mediated autophagy following paraquat exposure, our current investigation should shed some light toward better understanding of the role of autophagy in paraquat toxicity in heart damage. Further study is warranted to elucidate the therapeutic value of AMPK and AMPK-related autophagic signaling molecule in the management of paraquat-induced myopathic anomalies.

SUPPLEMENTARY DATA

Supplementary data are available online at http://toxsci.oxfordjournals.org/.

FUNDING

National Institute of Health/National Center for Research Resources (5P20RR016474); National Institute of Health/National Institute of General Medical Sciences (8P20GM103432).

REFERENCES

Alexi, T., Borlongan, C. V., Faull, R. L., Williams, C. E., Clark, R. G., Gluckman, P. D. and Hughes, P. E. (2000). Neuroprotective strategies for basal ganglia degeneration: Parkinson's and Huntington's diseases. *Prog. Neurobiol.* **60**, 409–470.

Bach, M., Larance, M., James, D. E. and Ramm, G. (2011). The serine/threonine kinase ULK1 is a target of multiple phosphorylation events. *Biochem. J.* **440**, 283–291.

Bus, J. S., Aust, S. D. and Gibson, J. E. (1976). Paraquat toxicity: Proposed mechanism of action involving lipid peroxidation. *Environ. Health Perspect.* **16**, 139–146.

Chan, Y. C., Chang, S. C., Hsuan, S. L., Chien, M. S., Lee, W. C., Kang, J. J., Wang, S. C. and Liao, J. W. (2007). Cardiovascular effects of herbicides and formulated adjuvants on isolated rat aorta and heart. *Toxicology In Vitro* **21**, 595–603.

Chan, E. Y., Longatti, A., McKnight, N. C. and Tooze, S. A. (2009). Kinase-inactivated ULK proteins inhibit autophagy via their conserved C-terminal domains using an Atg13-independent mechanism. *Mol. Cell. Biol.* **29**, 157–171.

Clark, D. G., McElligott, T. F. and Hurst, E. W. (1966). The toxicity of paraquat. *Br. J. Ind. Med.* **23**, 126–132.

Cristovao, A. C., Choi, D. H., Baltazar, G., Beal, M. F. and Kim, Y. S. (2009). The role of NADPH oxidase 1-derived reactive oxygen species in paraquat-mediated dopaminergic cell death. *Antioxid. Redox Signal.* **11**, 2105–2118.

Dagda, R. K., Das Banerjee, T. and Janda, E. (2013). How Parkinsonian toxins dysregulate the autophagy machinery. *Int. J. Mol. Sci.* **14**, 22163–22189.

Day, B. J. and Crapo, J. D. (1996). A metalloporphyrin superoxide dismutase mimetic protects against paraquat-induced lung injury in vivo. *Toxicol. Appl. Pharmacol.* **140**, 94–100.

Day, B. J., Hatch, A., Carstens, D. D. and Crapo, J. D. (1995). An easy and economical method to prepare cells for cytologic analyses. *J. Pharmacol. Toxicol. Methods* **34**, 57–62.

Efeyan, A. and Sabatini, D. M. (2010). mTOR and cancer: Many loops in one pathway. *Curr. Opin. Cell Biol.* **22**, 169–176.

Egan, D. F., Shackelford, D. B., Mihaylova, M. M., Gelino, S., Kohnz, R. A., Mair, W., Vasquez, D. S., Joshi, A., Gwinn, D. M., Taylor, R., *et al.* (2011). Phosphorylation of ULK1 (hATG1) by AMP-activated protein kinase connects energy sensing to mitophagy. *Science* **331**, 456–461.

Fumarola, C., Bonelli, M. A., Petronini, P. G. and Alfieri, R. R. (2014). Targeting PI3K/AKT/mTOR pathway in non small cell lung cancer. *Biochem. Pharmacol.*, **90**, 197–207.

Ganley, I. G., Lam du, H., Wang, J., Ding, X., Chen, S. and Jiang, X. (2009). ULK1.ATG13.FIP200 complex mediates mTOR signaling and is essential for autophagy. *J. Biol. Chem.* **284**, 12297–12305.

Garcia-Garcia, A., Anandhan, A., Burns, M., Chen, H., Zhou, Y. and Franco, R. (2013). Impairment of Atg5-dependent autophagic flux promotes paraquat- and MPP(+)-induced apoptosis but not rotenone or 6-hydroxydopamine toxicity. *Toxicol. Sci.* **136**, 166–182.

Ge, W., Zhang, Y., Han, X. and Ren, J. (2010). Cardiac-specific overexpression of catalase attenuates paraquat-induced myocardial geometric and contractile alteration: Role of ER stress. *Free Radic. Biol. Med.* **49**, 2068–2077.

Giri, S. N., Hollinger, M. A. and Schiedt, M. J. (1981). The effects of paraquat and superoxide dismutase on pulmonary vascular permeability and edema in mice. *Arch. Environ. Health* **36**, 149–154.

Gonzalez-Polo, R. A., Niso-Santano, M., Ortiz-Ortiz, M. A., Gomez-Martin, A., Moran, J. M., Garcia-Rubio, L., Francisco-Morcillo, J., Zaragoza, C., Soler, G. and Fuentes, J. M. (2007). Inhibition of paraquat-induced autophagy accelerates the apoptotic cell death in neuroblastoma SH-SY5Y cells. *Toxicol. Sci.* **97**, 448–458.

Gonzalez-Polo, R. A., Rodriguez-Martin, A., Moran, J. M., Niso, M., Soler, G. and Fuentes, J. M. (2004). Paraquat-induced apoptotic cell death in cerebellar granule cells. *Brain Res.* **1011**, 170–176.

Gottlieb, R. (2012). *Autophagy in Health and Disease*. Academic Press, London.

Guo, R. and Ren, J. (2012). Deficiency in AMPK attenuates ethanol-induced cardiac contractile dysfunction through inhibition of autophagosome formation. *Cardiovasc. Res.* **94**, 480–491.

Inoki, K., Zhu, T. and Guan, K. L. (2003). TSC2 mediates cellular energy response to control cell growth and survival. *Cell* **115**, 577–590.

Kassiotis, C., Ballal, K., Wellnitz, K., Vela, D., Gong, M., Salazar, R., Frazier, O. H. and Taegtmeyer, H. (2009). Markers of autophagy are downregulated in failing human heart after mechanical unloading. *Circulation* **120**(Suppl. 11), S191–S197.

Kim, J., Kundu, M., Viollet, B. and Guan, K. L. (2011). AMPK and mTOR regulate autophagy through direct phosphorylation of Ulk1. *Nat. Cell Biol.* **13**, 132–141.

Klionsky, D. J. and Emr, S. D. (2000). Autophagy as a regulated pathway of cellular degradation. *Science* **290**, 1717–1721.

Koo, J. R., Kim, J. C., Yoon, J. W., Kim, G. H., Jeon, R. W., Kim, H. J., Chae, D. W. and Noh, J. W. (2002). Failure of continuous venovenous hemofiltration to prevent death in paraquat poisoning. *Am. J. kidney Dis.* **39**, 55–59.

Kuma, A., Hatano, M., Matsui, M., Yamamoto, A., Nakaya, H., Yoshimori, T., Ohsumi, Y., Tokuhisa, T. and Mizushima, N. (2004). The role of autophagy during the early neonatal starvation period. *Nature* **432**, 1032–1036.

Lamming, D. W., Ye, L., Sabatini, D. M. and Baur, J. A. (2013). Rapalogs and mTOR inhibitors as anti-aging therapeutics. *J. Clin. Invest.* **123**, 980–989.

Lee, J. W., Park, S., Takahashi, Y. and Wang, H. G. (2010). The association of AMPK with ULK1 regulates autophagy. *PloS One* **5**, e15394.

Levine, B. and Klionsky, D. J. (2004). Development by self-digestion: Molecular mechanisms and biological functions of autophagy. *Dev. Cell* **6**, 463–477.

Liou, H. H., Tsai, M. C., Chen, C. J., Jeng, J. S., Chang, Y. C., Chen, S. Y. and Chen, R. C. (1997). Environmental risk factors and Parkinson's disease: A case-control study in Taiwan. *Neurology* **48**, 1583–1588.

Li, Q., Yang, X., Sreejayan, N. and Ren, J. (2007). Insulin-like growth factor I deficiency prolongs survival and antagonizes paraquat-induced cardiomyocyte dysfunction: Role of oxidative stress. *Rejuvenation Res.* **10**, 501–512.

Loffler, A. S., Alers, S., Dieterle, A. M., Keppeler, H., Franz-Wachtel, M., Kundu, M., Campbell, D. G., Wesselborg, S., Alessi, D. R. and Stork, B. (2011). Ulk1-mediated phosphorylation of AMPK constitutes a negative regulatory feedback loop. *Autophagy* **7**, 696–706.

Manning-Bog, A. B., McCormack, A. L., Li, J., Uversky, V. N., Fink, A. L. and Di Monte, D. A. (2002). The herbicide paraquat causes up-regulation and aggregation of alpha-synuclein in mice: Paraquat and alpha-synuclein. *J. Biol. Chem.* **277**, 1641–1644.

Manning-Bog, A. B., McCormack, A. L., Purisai, M. G., Bolin, L. M. and Di Monte, D. A. (2003). Alpha-synuclein overexpression protects against paraquat-induced neurodegeneration. *J. Neurosci.* **23**, 3095–3099.

McCormack, A. L., Atienza, J. G., Johnston, L. C., Andersen, J. K., Vu, S. and Di Monte, D. A. (2005). Role of oxidative stress in paraquat-induced dopaminergic cell degeneration. *J. Neurochem.* **93**, 1030–1037.

McCormack, A. L., Thiruchelvam, M., Manning-Bog, A. B., Thiffault, C., Langston, J. W., Cory-Slechta, D. A. and Di Monte, D. A. (2002). Environmental risk factors and Parkinson's disease: Selective degeneration of nigral dopaminergic neurons caused by the herbicide paraquat. *Neurobiol. Dis.* **10**, 119–127.

Musi, N., Hirshman, M. F., Arad, M., Xing, Y., Fujii, N., Pomerleau, J., Ahmad, F., Berul, C. I., Seidman, J. G., Tian, R., *et al.* (2005). Functional role of AMP-activated protein kinase in the heart during exercise. *FEBS Lett.* **579**, 2045–2050.

Mu, J., Brozinick, J. T., Jr, Valladares, O., Bucan, M. and Birnbaum, M. J. (2001). A role for AMP-activated protein kinase in contraction- and hypoxia-regulated glucose transport in skeletal muscle. *Mol. Cell* **7**, 1085–1094.

Nakai, A., Yamaguchi, O., Takeda, T., Higuchi, Y., Hikoso, S., Taniike, M., Omiya, S., Mizote, I., Matsumura, Y., Asahi, M., *et al.* (2007). The role of autophagy in cardiomyocytes in the basal state and in response to hemodynamic stress. *Nat. Med.* **13**, 619–624.

Nemchenko, A., Chiong, M., Turer, A., Lavandero, S. and Hill, J. A. (2011). Autophagy as a therapeutic target in cardiovascular disease. *J. Mol. Cell. Cardiol.* **51**, 584–593.

Niso-Santano, M., Gonzalez-Polo, R. A., Bravo-San Pedro, J. M., Gomez-Sanchez, R., Lastres-Becker, I., Ortiz-Ortiz, M. A., Soler, G., Moran, J. M., Cuadrado, A., Fuentes, J. M., *et al.* (2010). Activation of apoptosis signal-regulating kinase 1 is a key factor in paraquat-induced cell death: Modulation by the Nrf2/Trx axis. *Free Radic. Biol. Med.* **48**, 1370–1381.

Niso-Santano, M., Moran, J. M., Garcia-Rubio, L., Gomez-Martin, A., Gonzalez-Polo, R. A., Soler, G. and Fuentes, J. M. (2006). Low concentrations of paraquat induces early activation of extracellular signal-regulated kinase 1/2, protein kinase B, and c-Jun N-terminal kinase 1/2 pathways: Role of c-Jun N-terminal kinase in paraquat-induced cell death. *Toxicol. Sci.* **92**, 507–515.

Niso-Santano, M., Bravo-San Pedro, J. M., Gomez-Sanchez, R., Climent, V., Soler, G., Fuentes, J. M. and Gonzalez-Polo, R. A. (2011). ASK1 overexpression accelerates paraquat-induced autophagy via endoplasmic reticulum stress. *Toxicol. Sci.* **119**, 156–168.

Peng, J., Mao, X. O., Stevenson, F. F., Hsu, M. and Andersen, J. K. (2004). The herbicide paraquat induces dopaminergic nigral apoptosis through sustained activation of the JNK pathway. *J. Biol. Chem.* **279**, 32626–32632.

Prasad, K., Tarasewicz, E., Mathew, J., Strickland, P. A., Buckley, B.,

Richardson, J. R. and Richfield, E. K. (2009). Toxicokinetics and toxicodynamics of paraquat accumulation in mouse brain. *Exp. Neurol.* **215**, 358–367.

Ren, J., Babcock, S. A., Li, Q., Huff, A. F., Li, S. Y. and Doser, T. A. (2009). Aldehyde dehydrogenase-2 transgene ameliorates chronic alcohol ingestion-induced apoptosis in cerebral cortex. *Toxicol. Lett.* **187**, 149–156.

Ren, J., Privratsky, J. R., Yang, X., Dong, F. and Carlson, E. C. (2008). Metallothionein alleviates glutathione depletion-induced oxidative cardiomyopathy in murine hearts. *Crit. Care Med.* **36**, 2106–2116.

Russell, R. R. III, Li, J., Coven, D. L., Pypaert, M., Zechner, C., Palmeri, M., Giordano, F. J., Mu, J., Birnbaum, M. J. and Young, L. H. (2004). AMP-activated protein kinase mediates ischemic glucose uptake and prevents postischemic cardiac dysfunction, apoptosis, and injury. *J. Clin. Invest.* **114**, 495–503.

Sciarretta, S., Volpe, M. and Sadoshima, J. (2014). Mammalian target of rapamycin signaling in cardiac physiology and disease. *Circ. Res.* **114**, 549–564.

Tawara, T., Fukushima, T., Hojo, N., Isobe, A., Shiwaku, K., Setogawa, T. and Yamane, Y. (1996). Effects of paraquat on mitochondrial electron transport system and catecholamine contents in rat brain. *Arch. Toxicol.* **70**, 585–589.

Tripathi, D. N., Chowdhury, R., Trudel, L. J., Tee, A. R., Slack, R. S., Walker, C. L. and Wogan, G. N. (2013). Reactive nitrogen species regulate autophagy through ATM-AMPK-TSC2-mediated suppression of mTORC1. *Proc. Natl. Acad. Sci. U.S.A.* **110**, E2950–E2957.

Turdi, S., Kandadi, M. R., Zhao, J., Huff, A. F., Du, M. and Ren, J. (2011). Deficiency in AMP-activated protein kinase exaggerates high fat diet-induced cardiac hypertrophy and contractile dysfunction. *J. Mol. Cell. Cardiol.* **50**, 712–722.

Wills, J., Credle, J., Oaks, A. W., Duka, V., Lee, J. H., Jones, J. and Sidhu, A. (2012). Paraquat, but not maneb, induces synucleinopathy and tauopathy in striata of mice through inhibition of proteasomal and autophagic pathways. *PloS One* **7**, e30745.

Wullschleger, S., Loewith, R. and Hall, M. N. (2006). TOR signaling in growth and metabolism. *Cell* **124**, 471–484.

Xie, M., Morales, C. R., Lavandero, S. and Hill, J. A. (2011). Tuning flux: Autophagy as a target of heart disease therapy. *Curr. Opin. Cardiol.* **26**, 216–222.

Xing, Y., Musi, N., Fujii, N., Zou, L., Luptak, I., Hirshman, M. F., Goodyear, L. J. and Tian, R. (2003). Glucose metabolism and energy homeostasis in mouse hearts overexpressing dominant negative alpha2 subunit of AMP-activated protein kinase. *J. Biol. Chem.* **278**, 28372–28377.

Xu, X., Bucala, R. and Ren, J. (2013a). Macrophage migration inhibitory factor deficiency augments doxorubicin-induced cardiomyopathy. *J. Am. Heart Assoc.* **2**, e000439.

Xu, X., Hua, Y., Nair, S., Zhang, Y. and Ren, J. (2013b). Akt2 knockout preserves cardiac function in high-fat diet-induced obesity by rescuing cardiac autophagosome maturation. *J. Mol. Cell Biol.* **5**, 61–63.

Xu, X., Roe, N. D., Weiser-Evans, M. C. and Ren, J. (2014). Inhibition of mammalian target of rapamycin with rapamycin reverses hypertrophic cardiomyopathy in mice with cardiomyocyte-specific knockout of PTEN. *Hypertension* **63**, 729–739.

Yuan, H., Perry, C. N., Huang, C., Iwai-Kanai, E., Carreira, R. S., Glembotski, C. C. and Gottlieb, R. A. (2009). LPS-induced autophagy is mediated by oxidative signaling in cardiomyocytes and is associated with cytoprotection. *Am. J. Physiol. Heart Circ. Physiol.* **296**, H470–H479.